J Neurophysiol 102: 1254–1264, 2009.
First published June 24, 2009; doi:10.1152/jn.00346.2009.

The Influence of Neuroactive Steroid Lipophilicity on $GABA_A$ Receptor Modulation: Evidence for a Low-Affinity Interaction

Mariangela Chisari,[1] Lawrence N. Eisenman,[3] Kathiresan Krishnan,[2] Achintya K. Bandyopadhyaya,[2] Cunde Wang,[2] Amanda Taylor,[1] Ann Benz,[1] Douglas F. Covey,[2] Charles F. Zorumski,[1,4] and Steven Mennerick[1,4]

[1]*Departments of Psychiatry,* [2]*Developmental Biology,* [3]*Neurology, and* [4]*Anatomy and Neurobiology, Washington University School of Medicine, St. Louis, Missouri*

Submitted 17 April 2009; accepted in final form 16 June 2009

Chisari M, Eisenman LN, Krishnan K, Bandyopadhyaya AK, Wang C, Taylor A, Benz A, Covey DF, Zorumski CF, Mennerick S. The influence of neuroactive steroid lipophilicity on $GABA_A$ receptor modulation: evidence for a low-affinity interaction. *J Neurophysiol* 102: 1254–1264, 2009. First published June 24, 2009; doi:10.1152/jn.00346.2009. Anesthetic steroids with actions at γ-aminobutyric acid type A receptors ($GABA_A$Rs) may access transmembrane domain binding site(s) directly from the plasma cell membrane. Accordingly, the effective concentration in lipid phase and the ability of the steroid to meet pharmacophore requirements for activity will both contribute to observed steady-state potency. Furthermore, onset and offset of receptor effects may be rate limited by lipid partitioning. Here we show that several GABA-active steroids, including naturally occurring neurosteroids, of different lipophilicity differ in kinetics and potency at $GABA_A$Rs. The hydrophobicity ranking predicted relative potency of $GABA_A$R potentiation and predicted current offset kinetics. Kinetic offset differences among steroids were largely eliminated by γ-cyclodextrin, a scavenger of unbound steroid, suggesting that affinity differences among the analogues are dwarfed by the contributions of nonspecific accumulation. A 7-nitrobenz-2-oxa-1,3-diazole (NBD)–tagged fluorescent analogue of the low-lipophilicity alphaxalone (C17-NBD-alphaxalone) exhibited faster nonspecific accumulation and departitioning than those of a fluorescent analogue of the high-lipophilicity (3α,5α)-3-hydroxypregnan-20-one (C17-NBD-3α5αA). These differences were paralleled by differences in potentiation of $GABA_A$R function. The enantiomer of C17-NBD-3α5αA, which does not satisfy pharmacophore requirements for steroid potentiation, exhibited identical fluorescence kinetics and distribution to C17-NBD-3α5αA, but was inactive at $GABA_A$Rs. Simple simulations supported our major findings, which suggest that neurosteroid binding affinity is low. Therefore both specific (e.g., fulfilling pharmacophore requirements) and nonspecific (e.g., lipid solubility) properties contribute to the potency and longevity of anesthetic steroid action.

INTRODUCTION

Neurosteroids are possible endogenous modulators of neuronal activity (Akk et al. 2007; Belelli et al. 2006) and potential anesthetic, neuroprotective, and anxiolytic drugs (Gasior et al. 1999; Zorumski et al. 2000). These actions probably derive from potent and efficacious enhancement of γ-aminobutyric acid type A receptor ($GABA_A$R)–mediated currents. Two naturally occurring neurosteroids, (3α,5α)-3-hydroxypregnan-20-one (3α5αP) and (3α,5α)-3,21-dihydroxypregnan-20-one (3α5αTHDOC) both potentiate GABA-gated currents in the mid-nanomolar to micromolar concentration range. These two steroids have typically been used interchangeably to assay neurosteroid effects under the assumption that the steroids share essential properties such as potency and kinetics of action. A third widely used neurosteroid analogue, which enhances $GABA_A$R-mediated current, is (3α,5α)-3-hydroxypregnane-11,20-dione (alphaxalone), the 11-keto derivative of 3α5αP. Alphaxalone is an active component of the intravenous anesthetic Althesin (Gasior et al. 1999). The 11-keto derivative of 3α5αTHDOC is (3α,5α)-3,21-dihydroxypregnane-11,20-dione (alphadolone). Alphadolone 21-acetate is used in 1:3 ratio with alphaxalone as a component of Althesin to improve solubility of alphaxalone, although alphadolone may have anesthetic properties by itself (Nadeson and Goodchild 2001).

Recent electrophysiology, imaging, and molecular biological/structural evidence suggest that the steroid binding site on the $GABA_A$R lies within the transmembrane domains of the receptor (Akk et al. 2005; Hosie et al. 2006, 2009; Li et al. 2007; Shu et al. 2004). If so, then membrane concentrations of steroid, rather than aqueous concentrations, are most relevant for GABAR modulation. An important prediction of this hypothesis is that steroid analogues with weaker lipophilicity should show weaker potentiating ability than that of analogues with higher lipophilicity, assuming that any pharmacophore differences among the comparators are small relative to lipophilicity contributions. Given a relatively similar binding affinity, a higher potency would be predicted for more lipophilic steroids because for a given free aqueous concentration (the measured independent variable in potency estimates), a higher membrane concentration (the relevant "free" concentration experienced by the receptor) would be achieved than that for a less lipophilic compound. If this prediction holds, it would have important implications for future drug design. In addition if natural steroids have different lipophilicity and—by extension—potency, then this finding would have important implications for the physiological relevance of the steroids.

We examined the lipophilicity of the four neurosteroid analogues mentioned earlier. Importantly, two widely assumed critical features of the pharmacophore were held constant in these analogues: a 3α-hydroxy substituent and a methylketone at carbon 17. Predicted log P values differed by nearly 2 log P units, offering an opportunity to test the above-cited predictions, under the initial assumption that binding affinity is similar among the analogues. The potency and functional longevity of the analogues varied with their lipophilicity and longevity was strongly reduced in the most lipophilic com-

Address for reprint requests and other correspondence: S. Mennerick, Department of Psychiatry, Washington University School of Medicine, 660 South Euclid Avenue, Box 8134, St. Louis, MO 63110 (E-mail: menneris@psychiatry.wustl.edu).

pounds when steroid removal was sped up, with brief application of γ-cyclodextrin (γCDX) to sequester steroids from the plasma membrane (Adam et al. 2002; de Boer et al. 2006; Shu et al. 2004). The similarity of behavior among the compounds in the presence of a steroid scavenger strongly suggests that physiological differences among the steroids arise most strongly from nonspecific accumulation of unbound steroid; affinity and pharmacophore differences contribute much less. Fluorescent analogues of 3α5αP (C17-7-nitrobenz-2-oxa-1,3-diazole [NBD]-3α5αA) and of alphaxalone (C17-NBD-alphaxalone) showed the expected differences in perimembrane and intracellular fluorescence accumulation as well as $GABA_AR$ potentiating actions. Because the replacement of the carbon 17 methylketone substituent results in a systematic nomenclature change from the pregnane steroid class to the androstane steroid class, we abbreviate the fluorescent 3α5αP analogue C17-NBD-3α5αA. In addition to lipophilicity contributions, other experiments support the importance of the pharmacophore. A fluorescent enantiomer of 3α5αP (*ent*-C17-NBD-3α5αA) was essentially inactive at $GABA_ARs$ while exhibiting cellular fluorescence indistinguishable from that of the natural enantiomer. Simple simulations support the idea that for a transmembrane binding site, potency and kinetics will both be strongly influenced by nonspecific accumulation. Our results suggest that steroid binding affinity is low despite high potency. We discuss the relevance of our findings to neurosteroid signaling and to drug design.

METHODS

Hippocampal cultures

Primary cultures were prepared from postnatal day 0 (P0) to P3 rat pups as previously described (Shu et al. 2004). Hippocampi were removed from isoflurane-anesthetized rats and were cut into 500-μm-thick slices. The hippocampal slices were digested with 1 mg/ml papain in oxygenated Leibovitz L-15 medium (Invitrogen, Gaithersburg, MD), followed by mechanical trituration in modified Eagle's medium (Invitrogen) containing 5% horse serum, 5% fetal calf serum, 17 mM D-glucose, 400 μM glutamine, 50 U/ml penicillin, and 50 μg/ml streptomycin. Cells were plated in modified Eagle's medium at a density of about 650 cells/mm^2 as mass cultures (onto 25-mm cover glasses for imaging experiments) or 100 cells/mm^2 on microdots of collagen as "microisland" cultures (onto 35-mm plastic culture dishes for electrophysiology experiments). Both cover glasses and plastic dishes were precoated with collagen microdroplets sprayed on a layer of 0.15% agarose. Cultures were maintained at 37°C in a humidified incubator with 5% CO_2-95% air. The antimitotic cytosine arabinoside (6.7 μM) was added 3–4 days after plating to stop glial proliferation. At 4–5 days after plating, half the culture medium was replaced with Neurobasal medium (Invitrogen) plus B27 supplement (Invitrogen).

Culture electrophysiology

Whole cell recordings from hippocampal neuron cultures (microisland) were performed 7–12 days following plating using an Axopatch 200B amplifier (Molecular Devices, Sunnyvale, CA). Cells were transferred from culture medium to an extracellular recording solution containing (in mM): 138 NaCl, 4 KCl, 2 $CaCl_2$, 1 $MgCl_2$, 10 glucose, 10 HEPES, 0.001 2,3-dihydroxy-6-nitro-7-sulfonyl-benzo[f]quinoxaline (NBQX), and 0.01 D-2-amino-5-phosphonovalerate (D-APV) at pH 7.25. Patch pipettes were filled with an internal solution containing (in mM): 130 cesium methanesulfonate, 4 NaCl, 5 EGTA, 0.5 $CaCl_2$, and 10 HEPES at pH 7.25. When filled with this solution pipette tip resistance was 4–6 MΩ. Cells were clamped at −20 mV. Access resistance (8–20 MΩ) was not compensated. Drug applications were made with a multibarrel, gravity-driven local perfusion system. The estimated solution exchange times were 120 ± 14 ms (10–90% rise), measured by the change in junction currents at the tip of an open patch pipette. Experiments were performed at room temperature.

Oocyte expression studies

Stage V–VI oocytes were harvested from sexually mature female *Xenopus laevis* (Xenopus One, Northland, MI) under 0.1% 3-aminobenzoic acid ethyl ester anesthesia, according to protocols approved by the Washington University Animal Studies Committee. Oocytes were defolliculated by shaking for 20 min at 37°C in collagenase (2 mg/ml) dissolved in calcium-free solution containing (in mM): 96 NaCl, 2 KCl, 1 $MgCl_2$, and 5 HEPES at pH 7.4. Capped mRNA, encoding rat $GABA_AR$ α1, β2, and γ2L subunits was transcribed in vitro using the mMESSAGE mMACHINE Kit (Ambion, Austin, TX) from linearized pBluescript vectors containing receptor coding regions. Subunit transcripts were injected in equal parts (20–40 ng total RNA) 8–24 h following defolliculation. Oocytes were incubated ≤5 days at 18°C in ND96 medium containing (in mM): 96 NaCl, 1 KCl, 1 $MgCl_2$, 2 $CaCl_2$, and 10 HEPES at pH 7.4, supplemented with pyruvate (5 mM), penicillin (100 U/ml), streptomycin (100 μg/ml), and gentamycin (50 μg/ml).

Oocyte electrophysiology

Two-electrode voltage-clamp experiments were performed with a Warner OC725 amplifier (Warner Instruments, Hamden, CT) 2–5 days following RNA injection. The extracellular recording solution was ND96 medium with no supplements. Intracellular recording pipettes were filled with 3 M KCl and had open-tip resistances of 1 MΩ. Drugs were applied from a common tip via a gravity-driven multibarrel delivery system. Drugs were coapplied with no preapplication period. Cells were voltage-clamped at −70 mV for all experiments and the peak current was measured for quantification of current amplitudes.

Image acquisition and processing

Live cell imaging experiments of fluorescent steroids were performed with a C1 scanning confocal laser attached to an inverted TE2000 microscope (Nikon, Melville, NY) using a ×40 air objective (numerical aperture, 0.95). Cover glasses with high-density neuronal cultures (7–15 days after plating) were mounted in an open round bath chamber (Warner Instruments) and maintained in the external solution described for electrophysiology experiments. Cells were labeled with 5 μg/ml CellMask Orange plasma membrane stain (Invitrogen) for 5 min at 37°C. Drugs were applied using a multibarrel, gravity-driven local perfusion system. Experiments were performed at room temperature. NBD-tagged steroids were imaged with an argon laser line for excitation at 488 nm with a 515/30-nm emission filter. Images of cells labeled with CellMask Orange were acquired using a Green HeNe laser line for excitation at 543 nm (590/50-nm emission filter). Gain settings, zoom, and field size parameters were kept constant for all live cell imaging experiments. Images were acquired with Z-C1 software (Nikon) and then processed with MetaMorph software (Molecular Devices, Downingtown, PA). For display, image brightness and contrast were altered equally for the entire series of images using MetaMorph to promote clarity of fluorescence visualization. Intrinsic pixel intensity values were not altered by these changes.

Data analysis and statistical procedures

Calculations of log P were made using on-line log P calculators (Marvin: http://www.chemaxon.com/demosite/marvin/index.html;

ALOGPS: http://www.vcclab.org/lab/alogps/). In the case of one test steroid (androsterone) measured log P values are available. The measured log P value compared favorably with the average calculated log P value (3.69 measured vs. 3.61 ± 0.1 average calculated). Data acquisition and analysis were performed with pCLAMP 9.0 software (Molecular Devices, Union City, CA). Data plotting and curve fitting were performed with Prism 5.01 software (GraphPad, San Diego, CA). Curve fitting was performed on potentiation values calculated as (M − G)/G, where M is the response in the presence of GABA + modulator and G is the response to GABA alone. Empirical fits to concentration–response relationships were achieved using a least-squares minimization to the Hill equation: $B_{max}[X^h/(EC_{50}^h + X^h)]$, where B_{max} is the maximum potentiation, h is the Hill coefficient, EC_{50} is the concentration of steroid producing 50% of maximum potentiation, and X is the test steroid concentration. For statistical comparisons among compounds, we consider the values derived from fits to individual cells to be most valid because this method better takes into account cell-to-cell variability. All statistical comparisons (e.g., Figs. 2*F* and 3*F*) were performed on EC_{50} values derived from fits to individual cells. For display, solid lines shown in Figs. 2 and 3 are Hill equation fits to the averaged experimental data. There was good agreement between fits derived from the two methods. EC_{50} values varied by only 28.3 ± 22.9% between the two methods. Rise and decay times in electrophysiology experiments were measured using a 10–90% time. For imaging experiments, the time to reach half the intensity value (for both onset and offset times) was calculated ($t_{1/2}$). The fluorescence in each compartment was normalized to the last point of steroid application (treated as 1), immediately before saline wash, to emphasize time course differences. Data are presented in the text and figures as mean ± SE. Statistical differences were determined using Student's two-tailed *t*-test.

Simulations

Simulations were run with NEURON version 7.0 (http://www.neuron.yale.edu/). The kinetic scheme is given in Fig. 9*A*. Other simulation details are given in the Supplemental text and Supplemental Table S1.[1]

Drugs, chemicals, and other materials

3α5αTHDOC and alphadolone were from Steraloids (Newport, RI). 3α5αP, alphaxalone, and other drugs were from Sigma (St Louis, MO). Fluorescent steroids were synthesized using 7-nitrobenz-2-oxa-1,3-diazole (NBD) as fluorophore and replacing the methyl ketone at carbon 17 with the fluorescent group. Multistep synthetic procedures were used to prepare fluorescent steroids and their structures were confirmed by spectroscopic properties (infrared spectroscopy and both proton and carbon nuclear magnetic resonance spectroscopy). Thin-layer chromatography and elemental analysis were used to determine the purity of these compounds. Steroids were prepared as stock solutions in dimethylsulfoxide (DMSO). Final DMSO concentration was <0.3% and solutions were matched for DMSO concentration.

RESULTS

Behavior of commonly used steroids with differing log P values

If membrane partitioning is important for steroids to find their site on the $GABA_AR$, steroid structural attributes that influence overall lipophilicity may affect steroid potency and time course of action, assuming that these differences are large relative to affinity differences. Because calculated log P values can vary quite widely with different algorithms, we used the average log P estimates from 11 different algorithms (Fig. 1; see METHODS). Interestingly, the most commonly used neurosteroids/neurosteroid analogues varied over a range of nearly two units in average estimated log P (Fig. 1). These included the naturally occurring neurosteroids 3α5αP and 3α5αTHDOC and the synthetic analogues alphaxalone and alphadolone. Average calculated log P values were 3α5αP: 4.2 ± 0.1; 3α5αTHDOC: 3.5 ± 0.1; alphaxalone: 3.1 ± 0.1; alphadolone: 2.3 ± 0.1. (Fig. 1*G*). To help us explore accumulation of steroids in cellular compartments, we also prepared fluorescently tagged

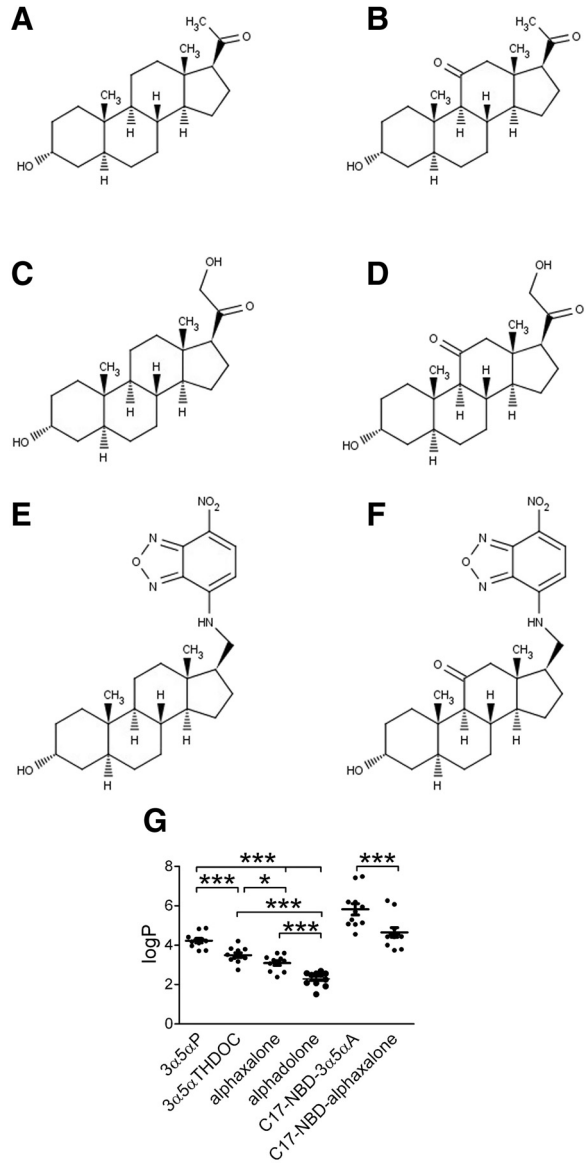

FIG. 1. Structures and predicted lipophilicity of natural and synthetic steroid analogues that potentiate γ-aminobutyric acid type A ($GABA_A$) currents. *A*: 3α5αP; *B*: alphaxalone; *C*: 3α5αTHDOC; *D*: alphadolone. 3α5αP and 3α5αTHDOC are natural neurosteroids. Alphaxalone and alphadolone are synthetic analogues. *E* and *F*: synthetic neuroactive steroid analogues with a fluorescent substituent (NBD) at carbon 17, C17-NBD-3α5αA (*E*) and C17-NBD-alphaxalone (*F*). *G*: estimated partition coefficients (log P) for each steroid. Values were calculated using 11 different algorithms and are shown as means ± SE, $*P < 0.05$, $***P < 0.0001$ (paired *t*-test). Alphadolone, (3α,5α)-3,21-dihydroxypregnane-11,20-dione; alphaxalone, (3α,5α)-3-hydroxypregnane-11,20-dione; 3α5αP, (3α,5α)-3-hydroxypregnan-20-one; 3α5αTHDOC, (3α,5α)-3,21-dihydroxypregnan-20-one; NBD, 7-nitrobenz-2-oxa-1,3-diazole.

[1] The online version of this article contains supplemental data.

analogues at carbon 17, allowing us to compare analogues with and without a ketone at C11. It is important to note that removal of the methyl ketone at carbon 17 and replacement with the NBD group significantly increased the estimated log P values over that of the parent compound, but a relative difference of approximately one log P unit, imparted by the ketone at carbon 11, was preserved (Fig. 1*G*).

To test the possible physiological implications of the log P differences, we first examined the concentration–response characteristics of 3α5αP (0.1–10 μM), 3α5αTHDOC (0.3–30 μM), alphaxalone (0.3–30 μM), and alphadolone (3–300 μM). We evaluated these characteristics in *Xenopus laevis* oocytes expressing an α1β2γ2L subunit combination (Fig. 2). We found that 3α5αP, the steroid with the highest calculated log P, exhibited the highest potency for $GABA_AR$ potentiation, and the rank order of potency over the four compounds correlated with log P estimates (Fig. 2*F*). The estimate for 3α5αP potency (EC_{50}) was comparable to that of our previously published results (Mennerick et al. 2004).

Because it appeared that substitutions at carbon 11 are qualitatively well tolerated, we also examined an additional steroid with an 11β-benzyloxy substituent (not commercially available) that extended our log P range further in the lipophilic direction. ZCM41 (Shu et al. 2004) has a calculated log P value of 5.4 as a result of a benzyloxy substitution at position 11 (Supplemental Fig. S1). We tested the EC_{50} in oocytes and estimated an EC_{50} of 0.1 μM. When added to the plot of Fig. 2*F*, it extends the relationship between log P and EC_{50} (Supplemental Fig. S1).

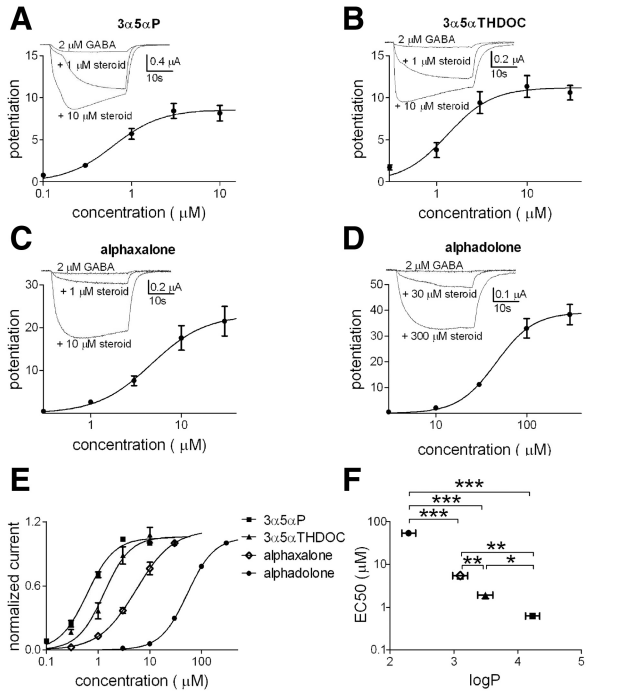

FIG. 2. Evaluation of steroid potentiation on $GABA_A$ receptors ($GABA_ARs$) in *Xenopus laevis* oocytes. Increasing concentrations of 3α5αP (*A*, 0.1–10 μM, $n = 7$), 3α5αTHDOC (*B*, 0.3–30 μM, $n = 17$), alphaxalone (*C*, 0.3–30 μM, $n = 16$), and alphadolone (*D*, 3–300 μM, $n = 4$) were applied to *Xenopus laevis* oocytes expressing rat α1β2γ2L $GABA_AR$ subunits. The concentration–response curves were obtained in the presence of 2 μM GABA and potentiated responses were expressed relative to the GABA response in the absence of steroid. For display purposes, the lines represent fits of the Hill equation to the averaged data points shown in the figure. Parameters from the summary fits for 3α5αP, 3α5αTHDOC, alphaxalone, and alphadolone, respectively, were EC_{50} (the concentration of steroid producing 50% of maximum potentiation): 0.6, 1.3, 4.6, and 45.9 μM; Hill coefficient: 1.6, 1.8, 1.5, and 2.1. *E*: concentration–response curves of the steroids were normalized to the individual maximum potentiation to facilitate comparison of shapes and EC_{50} values. *F*: summary EC_{50} values from fits to the individual oocytes. The EC_{50} values for each steroid are shown as a function of log P. Values are means ± SE; $*P < 0.05$, $**P < 0.01$, $***P < 0.0001$ (unpaired *t*-test).

For further evaluation, we examined dissociated cultures of hippocampal neurons, so that solution exchange times could be controlled more rapidly and precisely. A similar rank order of steroid potency was observed in cultures as in oocytes among the widely available analogues (Fig. 3). For concentration–response evaluation in neurons the range of neurosteroid concentration was modified (3α5αP, 0.03–3 μM; 3α5αTHDOC, 0.3–10 μM; alphaxalone, 0.1–30 μM; alphadolone, 1–100 μM). It should be noted that although we used a long drug exposure time (20 s) to try to allow effects to achieve steady state, in some neurons it was apparent that at the lowest concentration of 3α5αP, a steady state had not been reached (Fig. 3*A*). When we doubled the length of exposure to 30 nM 3α5αP, potentiation grew from 5.11 ± 3.1 at 20 s to 7.31 ± 3.3 at 40 s ($n = 3$). Therefore it is possible that potency is slightly higher for 3α5αP than Fig. 3 suggests (Li et al. 2007).

In these protocols it was apparent that offset times of potentiated responses, on removal of steroid and return to a solution of GABA alone, were correlated with calculated compound lipophilicity (Fig. 3, *A–D*, *traces*). With typical drug–receptor interactions, the current offset on aqueous drug removal inversely correlates with compound affinity for the receptor (Colquhoun et al. 1977; Lester and Jahr 1992; but see Jones et al. 1998). Further, for typical ligand–receptor interactions, the current offset time should not depend on aqueous compound concentration, unlike the rise time of the potentiation effect. However, in the case of steroid interactions with $GABA_ARs$, we have previously suggested that nonspecific membrane/cellular departitioning affects the longevity of steroid actions (Akk et al. 2005; Shu et al. 2004). Comparison of steroid traces with equimolar concentration (1 μM) highlighted distinct decay kinetics for the three compounds (Fig. 4*A*). Alphadolone was not included in this evaluation because the potentiation with 1 μM was weak (Fig. 3*D*). With equimolar concentrations of the three analogues, we found no significant difference in rise times among the compounds (Fig. 4*A*, *middle*). Offset time was significantly slowed with increasing lipophilicity of the analogues (Fig. 4*A*, *right*).

Because the EC_{50} value for 3α5αP was the lowest compared with other steroids, the slow offset in Fig. 4*A* might be caused by technical problems in washing away steroid concentrations in excess of the compound's EC_{50}. To avoid this potential problem, we examined decay kinetics for the three steroid analogues at concentrations close to each compound's EC_{20} for steady-state $GABA_AR$ potentiation (3α5αP, 0.05 μM; 3α5αTHDOC, 0.3 μM; alphaxalone, 0.85 μM). Exemplar traces from this comparison are shown in Fig. 4*B*. 3α5αP still clearly exhibited slower decay kinetics than that of the other neuroactive steroids.

The rise time of the most lipophilic steroid 3α5αP was also notably slower at the EC_{20} concentrations (Fig. 4*B*). For a simple model of ligand–receptor interaction, at very low agonist concentrations, the rate constant of approach to equilibrium will be dominated by the agonist dissociation rate ($k_{obs} =$

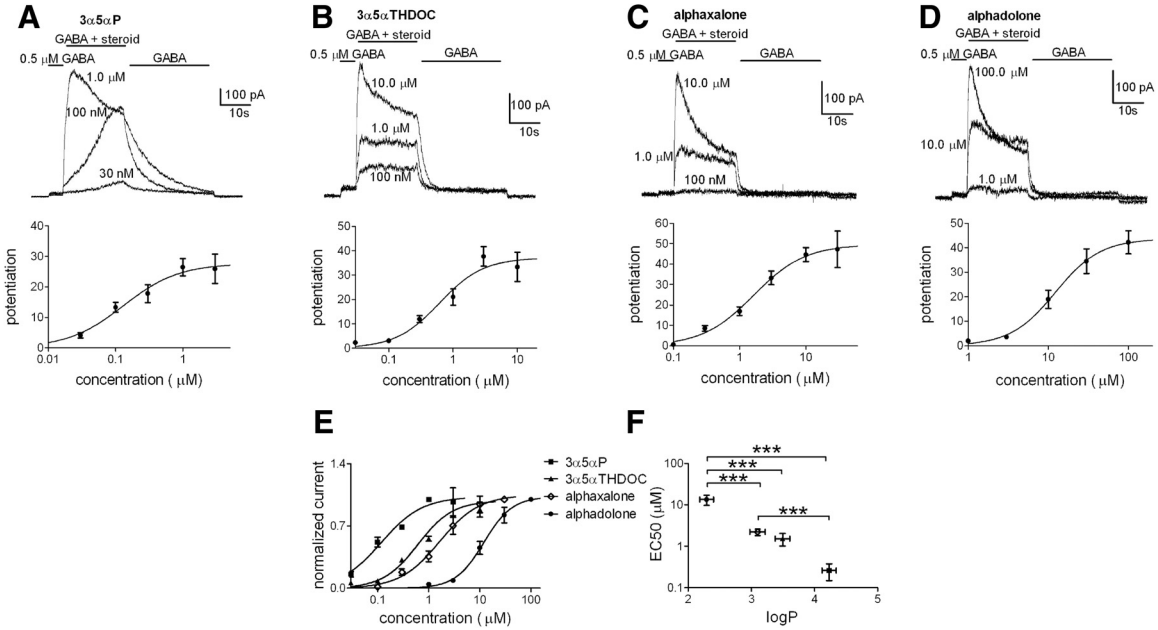

FIG. 3. Evaluation of steroid potentiation on $GABA_A$Rs in hippocampal neurons. Steroid potentiation traces (*top panels*) of increasing concentrations of 3α5αP (*A*, 0.03–3 μM, $n = 11$), 3α5αTHDOC (*B*, 0.03–10 μM, $n = 16$), alphaxalone (*C*, 0.1–30 μM, $n = 17$), and alphadolone (*D*, 1–100 μM, $n = 4$), applied to neuronal cultures. The concentration–response curves (*A–D*, *bottom panels*) were obtained in the presence of 0.5 μM GABA and potentiated responses were normalized to the first GABA application (see METHODS). For display purposes, the lines represent fits of the Hill equation to the averaged data points shown in the figure. Parameters from the summary fits for 3α5αP, 3α5αTHDOC, alphaxalone, and alphadolone, respectively, were EC_{50}: 0.3, 1.5, 2.2, and 13.4 μM; Hill coefficient: 1.1, 1.3, 1.1, and 1.5. *E*: data for each steroid were normalized to the individual maximum potentiation to facilitate potency comparisons. *F*: the estimated EC_{50} values for the steroids from fits to the individual cells are shown as a function of the corresponding log P. Values are means ± SE; $***P < 0.0001$ (unpaired *t*-test). The comparison of 3α5αTHDOC vs. 3α5αP showed a significant difference only with a one-tailed *t*-test ($P < 0.05$).

k_f[Agonist] + k_b, where k_{obs} is the observed rate constant of approach to equilibrium, k_f is the forward rate constant of ligand–receptor complex formation, and k_b is the backward rate constant) (Gutfreund 1995). Therefore the slow rise of 3α5αP qualitatively supports the idea that 3α5αP has either a slow dissociation rate from the receptor or a slow dissociation rate from membrane, if indeed lipophilicity is important for steroid access to the receptor. The rate of rise of 3α5αP effect was clearly nonexponential (Figs. 3*A* and 4*B*), indicating that factors other than simple ligand–receptor binding participate in the approach toward steady-state potentiation.

Taken together, the results described thus far could suggest that steroid lipophilicity participates in potency and longevity of steroid actions at $GABA_A$Rs. Alternatively, the correlation of lipophilicity with potency and longevity could be a coincidence and the analogues may simply differ in their intrinsic affinity for a binding site on the receptor (Colquhoun et al. 1977; Lester and Jahr 1992). For instance, over a database of steroid structural analogues accumulated by our group, we found only a weak correlation between lipophilicity and activity of 0.1 μM compound on GABARs in oocytes (Supplemental Fig. S2). This likely is because some of the structural

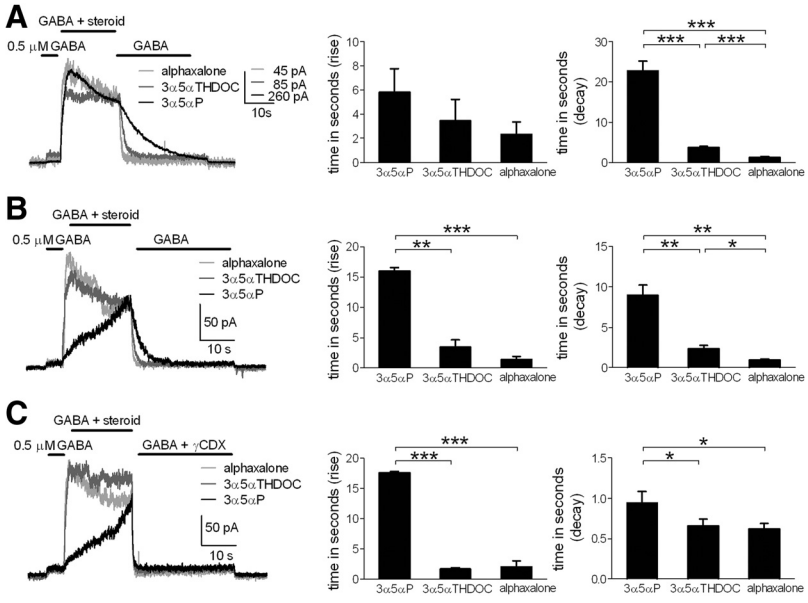

FIG. 4. Onset and offset kinetics of different steroid analogues in neuronal cultures. *A*: representative traces of steroid potentiation yielded by equimolar analogue concentration (1 μM). Compounds were coapplied with GABA (0.5 μM) after a GABA preapplication. Comparisons of 10–90% rise and decay times are shown (bar diagrams). Values are means ± SE (3α5αP, $n = 5$; 3α5αTHDOC, $n = 6$; alphaxalone, $n = 7$); $***P < 0.0001$ (unpaired *t*-test). There was no statistical difference in rise time among the 3 analogues at 1 μM. *B*: representative traces of steroid potentiation determined by EC_{20} analogue concentration (0.05 μM, 3α5αP; 0.3 μM, 3α5αTHDOC; 0.85 μM, alphaxalone). Comparisons of rise and decay times are shown (bar diagrams). Values are means ± SE ($n = 5$); $*P < 0.05$, $**P < 0.01$, $***P < 0.0001$ (paired *t*-test). *C*: representative traces of steroid potentiation determined with EC_{20} concentration (0.05 μM, 3α5αP; 0.3 μM, 3α5αTHDOC; 0.85 μM, alphaxalone). Potentiation removal was determined by coapplication of 500 μM γCDX with 0.5 μM GABA. Comparisons of mean rise and decay times are shown (bar diagrams). Values are means ± SE ($n = 6$); $*P < 0.05$, $***P < 0.0001$ (paired *t*-test).

alterations affect the pharmacophore (in addition to lipophilicity), some affect lipophilicity with weak pharmacophore effects, and some may affect higher-order steroid behavior in membranes (Makriyannis et al. 2005).

If the affinity explanation for kinetic differences among the analogues in Figs. 1–3 is true, then the differences in potentiation offset time (for instance in the protocol shown in Fig. 4*B*) should not be affected by removing free, membrane-partitioned steroid with cyclodextrin molecules (Akk et al. 2005; Shu et al. 2004). We tested this prediction by including 500 μM γCDX in the wash solution along with GABA, following steroid exposure (Fig. 4*C*). We found that γCDX reduced offset times of the three steroids with the offset times of all three drugs now approaching the limit of aqueous solution exchange times (Fig. 4*C*). Alphaxalone and 3α5αTHDOC offset times were similar in the presence of γCDX, but 3α5αP was still slower compared with other steroids. Compared with 3α5αTHDOC and alphaxalone, 3α5αP offset times were 6.67 $\pm$ 1.3 and 7.9 $\pm$ 1.2 s slower, respectively, in the absence of γCDX and only 0.28 $\pm$ 0.1 and 0.32 $\pm$ 0.1 s slower in the presence of γCDX. Although these residual differences in the presence of γCDX could result from differences in the affinity of the various ligands for the receptor (structural differences that affect the pharmacophore), the largely equalized kinetics in the presence of the scavenger suggests that pharmacophore/affinity differences are dwarfed by CDX-sensitive nonspecific accumulation. γCDX did not affect the amplitude of the GABA response (Fig. 4*C*), consistent with our previous suggestions that this concentration of γCDX does not interfere directly with GABAR function (Akk et al. 2005; Shu et al. 2004, 2007; but see Pytel et al. 2006). In summary, this experiment supports the idea that variable lipophilicity explains much of the potency and kinetic differences among these steroid analogues.

Behavior of fluorescent analogues of alphaxalone and 3α5αP

As an additional empirical approach for testing whether nonspecific accumulation differs between steroid analogues with differing predicted membrane solubility, we examined NBD-tagged analogues of 3α5αP and of alphaxalone (see Fig. 1). For both compounds, biological activity ($GABA_AR$ potentiation) was retained despite removal of the methyl ketone and substitution of the NBD fluorophore at carbon 17. However, in oocyte screens we found that efficacy was reduced (Supplemental Fig. S3), consistent with the idea that tagging disrupted the pharmacophore (the methyl ketone at C17). Further, for the most lipophilic analogue (C17-NBD-3α5αA), it was difficult to obtain steady-state values because of extremely slow equilibration (see following text). Equimolar concentrations (0.5 μM) for both fluorescent compounds were used for most experiments. Consistent with the increase in lipophilicity expected as a result of tagging (Fig. 1), both fluorescent compounds exhibited slower kinetics than that of their untagged counterparts (Fig. 5 vs. Fig. 4). Potentiation by C17-NBD-3α5αA, the tagged analogue with higher predicted log P, rose and fell more slowly compared with C17-NBD-alphaxalone (Fig. 5*A*, *gray trace*, Fig. 5, *B* and *C*). Note that in Fig. 5*B* the decay times assigned for C17-NBD-3α5αA were often artificially reduced to 30 s, the limit of wash time, in cases where steroid effects had not decayed by the end of the wash period

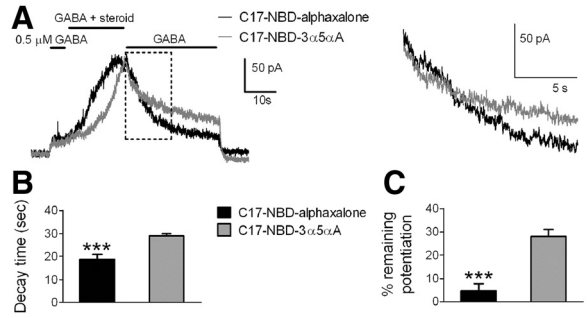

FIG. 5. Potentiation characteristics of C17-NBD fluorescent steroid analogues. *A*: representative traces of fluorescent steroid potentiation (*left*) and expanded detail of the boxed region during wash (*right*) determined at equimolar concentration (0.5 μM). Drugs were coapplied with GABA (0.5 μM) on hippocampal neurons. *B*: bar diagrams indicate decay times of tagged steroids. Values are means $\pm$ SE (n = 13); ***$P < 0.0001$ (paired t-test). Analysis was performed as described in METHODS. Since many cells (12/13 cells) treated with C17-NBD-3α5αA failed to fall to 10% of the peak potentiation by the end of the 30-s wash, a conservative time equal to the total washing time (30 s) was assigned for purposes of averaging. In these same 13 cells, potentiation in 3/13 treated with C17-NBD-alphaxalone failed to fall to 10% and a 30-s fall time was similarly assigned. *C*: bar diagrams indicate remaining potentiation of fluorescent steroids after 30-s wash with 0.5 μM GABA. Values are means $\pm$ SE (n = 13); ***$P < 0.0001$ (paired t-test).

(see Fig. 5 legend for description). As an alternative description of potentiation offset, residual potentiation was measured following the 30-s wash in GABA alone (Fig. 5*C*). Again, this analysis showed that C17-NBD-3α5αA potentiation was clearly more resistant to wash than C17-NBD-alphaxalone.

These observations predict that nonspecific accumulation should be slower to rise and more resistant to wash for the 3α5αP-tagged analogue than for the alphaxalone analogue. To test these predictions, we imaged cells during steroid exposures similar to those used for electrophysiology. We imaged both perimembrane (colocalized with CellMask Orange plasma membrane stain) and intracellular fluorescence in single confocal planes from individual neurons (Fig. 6*A*). We found that with a 40-s application, C17-NBD-alphaxalone seemed to approach a steady-state fluorescence, whereas C17-NBD-3α5αA fluorescence was clearly still on its ascendancy at the end of the 40-s exposure. Unexpectedly, perimembrane and especially intracellular fluorescence of C17-NBD-3α5αA often continued to increase beyond the initiation of wash, whereas C17-NBD-alphaxalone fluorescence began declining immediately on wash initiation (Fig. 6, *B* and *D*). This difference in behavior of the analogues was not the result of different effective concentrations. Raising the concentration of C17-NBD-alphaxalone 10-fold to 5 μM to account for lipophilicity differences between the analogues did not qualitatively alter the behavior on washout (Supplemental Fig. S4). Deep intracellular fluorescence remained high for C17-NBD-3α5αA, even after initiation of γCDX wash (Fig. 6*B*, arrows), although on γCDX wash, intracellular fluorescence began to decrease (Fig. 6*B*).

The imaging results broadly support the predictions from electrophysiology and suggest that C17-NBD-3α5αA is slower to accumulate (Fig. 6*E*) and more difficult to remove than C17-NBD-alphaxalone (Fig. 6, *D* and *F*). However, several details are difficult to reconcile. Perimembrane fluorescence of C17-NBD-3α5αA stayed relatively level on wash initiation, whereas GABA current potentiation began an immediate decay (Fig. 6*B* vs. Fig. 5*A*). Furthermore, intracellular fluorescence

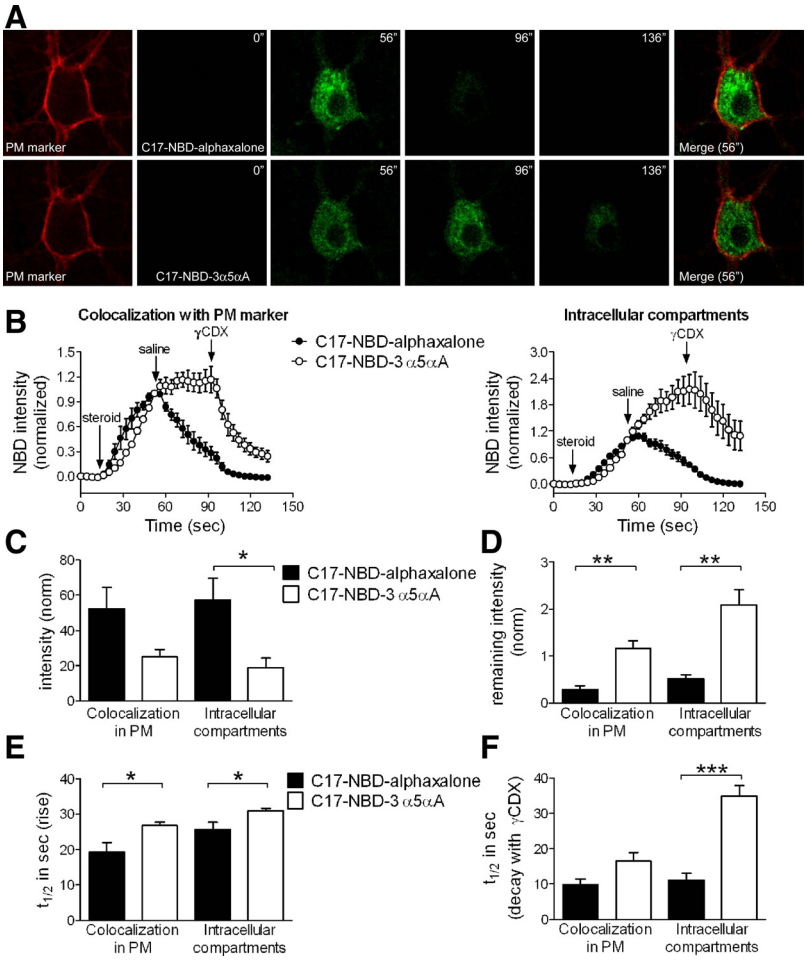

FIG. 6. Imaging and analysis of C17-NBD fluorescent steroid analogues. *A*: hippocampal neurons were stained with a plasma membrane (PM) marker (CellMask Orange) and NBD-tagged steroids (0.5 μM) were applied for 40 s. Washes with saline and then with 500 μM γ-cyclodextrin (γCDX) lasted for 40 s (each wash). Images were acquired with 4-s interval. NBD fluorescence was always higher for C17-NBD-alphaxalone (*A*, 56″) and wash with saline was sufficient to remove fluorescence (*A*, 96″). By contrast, C17-NBD-3α5αA was difficult to remove even after 40-s wash with 500 μM γCDX (*A*, 136″). Merged images use the NBD-steroid images from 56″. *B*: fluorescence intensities of selected regions were plotted over time. Intensity values are means ± SE (n = 6). The fluorescence in each compartment was normalized to the last point of steroid application, immediately before saline wash, to emphasize time course differences. Start points of steroid applications and washes are indicated. C17-NBD-3α5αA was not removed by saline and surprisingly exhibited a fluorescence increase in the intracellular compartment during wash with saline. The increase was not as evident in perimembrane regions associated with the plasma membrane marker. *C–F*: quantitative comparisons of C17-NBD analogues in both intracellular compartments and perimembrane regions. Values are means ± SE (n = 6). *C*: bar diagrams of normalized fluorescence intensities at the end of steroid application. *$P < 0.05$ (paired t-test). *D*: bar diagrams of normalized remaining fluorescence intensities after saline wash (before γCDX application). **$P < 0.01$ (paired t-test). *E*: bar diagrams of onset times using the time to reach half the intensity value measured at the end of steroid application ($t_{1/2}$). *$P < 0.05$ (paired t-test). *F*: bar diagrams of offset times during wash with 500 μM γCDX using the time to reach half the intensity value measured at the end of γCDX application ($t_{1/2}$). Note that the $t_{1/2}$ for intracellular fluorescence elimination is artificially truncated at the limit of the 40-s wash time. ***$P <$ 0.0001 (paired t-test).

continued to rise on wash (Fig. 6*B*, *right*). We suggest explanations for these discrepancies in the DISCUSSION.

Imaging experiments confirmed that higher lipophilicity influences the intracellular accumulation and elimination of different steroids. To test whether residual intracellular steroids might have an effect on GABAR function, we measured persisting potentiation after a 20-s saline wash. After application of C17-NBD-alphaxalone, using the same protocol shown in Fig. 5, neurons were reexposed to GABA alone following 20-s wash. We found no change compared with the original GABA response, either following 0.5 μM or 1 μM C17-NBD-alphaxalone exposures (Fig. 7, *A*, *right* and *C*). By contrast, after C17-NBD-3α5αA application (0.5 μM), the second exposure to GABA exhibited a residual potentiation (>threefold) over the original GABA response (Fig. 7, *B* and *C*).

We reasoned that if residual intracellular steroid is responsible for the prolonged C17-NBD-3α5αA effects, removal of superficial steroid with a brief γCDX wash should reveal a "rebound" potentiation as intracellular steroid reequilibrates with plasma membrane GABARs. Following potentiation of GABA currents, cells were washed with γCDX for 15 s to bring the response back to the original GABA-current level (Fig. 7, *D* and *E*). This indicated elimination of plasma membrane steroid. Removal of γCDX to a solution of GABA alone exhibited the predicted rebound potentiation for C17-NBD-3α5αA (Fig. 7*E*), but very little rebound for C17-NBD-alphaxalone (Fig. 7*D*) under the same conditions. The rebound for C17-NBD-3α5αA was 1.5-fold larger than that of C17-NBD-alphaxalone. Even in experiments using double the C17-NBD-alphaxalone concentration (1 μM), there was no further rebound on γCDX removal (Fig. 7, *D* and *F*). Testing parent compounds in a similar protocol, a rebound potentiation following brief γCDX wash was detected after exposure of neurons to 1 μM 3α5αP and not to 10 μM alphaxalone (1.8-fold larger) (Fig. 7*F*). These experiments suggested that trapped intracellular C17-NBD-3α5αA and 3α5αP, not immediately accessible to γCDX, can slowly reequilibrate with the plasma membrane and affect GABAR function. This offers a likely explanation for the wash-resistant component of C17-NBD-3α5αA potentiation.

Fluorescent enantiomers distinguish nonspecific from specific contributions

Intracellular accumulation of steroids shown by imaging experiments could represent active transport of steroid or could represent passive diffusion through the plasma membrane. If the first process is involved, we would expect that compound movement into the cell should exhibit enantioselectivity. This is because ligand interaction with proteins involves a "handedness" preference, given that proteins are made entirely of L-amino acids (Westover and Covey 2004). On the other hand, if steroid movement is entirely mediated by lipophilicity, we would expect no enantioselectivity (Alakoskela et al. 2007). To

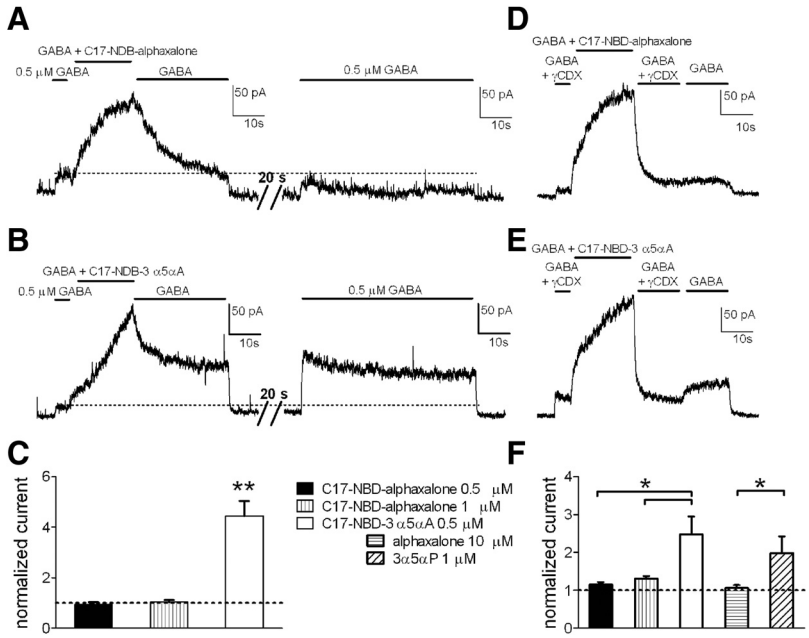

FIG. 7. Effects of intracellular accumulation of C17-NBD steroid analogues on GABA response potentiation in neurons. *A* and *B*: representative traces of GABA potentiation determined for 0.5 μM C17-NBD-alphaxalone (*A*, *left*) and 0.5 μM C17-NBD-3α5αA (*B*, *left*), followed by a 30-s wash in GABA alone, a 20-s wash in saline, and a reapplication of GABA alone (*A* and *B*, *right*) The GABA reapplication showed a larger residual current following C17-NBD-3α5αA potentiation. *C*: summary of effects over multiple cells treated as in *A* and *B*. Doubling the concentration of C17-NBD-alphaxalone (1 μM; middle bar) did not increase the response to a test GABA application. GABA responses to the second application are normalized to the first (original) GABA application (dotted horizontal line). Values are means ± SE (n = 10 for 0.5 μM C17-NBD-alphaxalone; n = 5 for 1 μM C17-NBD-alphaxalone; n = 11 for 0.5 μM C17-NBD-3α5αA); $^{**}P < 0.01$ (unpaired t-test). *D* and *E*: representative traces of GABA potentiation by C17-NBD-alphaxalone (*D*) and C17-NBD-3α5αA (*E*) (0.5 μM), applied with GABA (0.5 μM). To speed offset of potentiation, γCDX (500 μM) was added in the GABA solution and applied for 15 s following potentiation. GABA alone was then immediately reapplied for 15 s. In cells previously exposed to C17-NBD-3α5αA, a rebound potentiation reemerged. *F*: summary of multiple cells treated as in *D* and *E*. Increasing C17-NBD-alphaxalone concentration to 1 μM did not increase rebound potentiation following GABA reapplication. Nonfluorescent compounds (10 μM alphaxalone and 1 μM 3α5αP) were tested with a similar protocol using a 10- to 15-s γCDX wash; a summary for rebound potentiation is shown. Rebound potentiation was normalized to the first (original) GABA application (dotted horizontal line). Values are means ± SE (n = 7 for 0.5 μM C17-NBD-alphaxalone; n = 6 for 1 μM C17-NBD-alphaxalone; n = 6 for 0.5 μM C17-NBD-3α5αA, n = 9 for 10 μM alphaxalone, n = 9 for 1 μM 3α5αP); $^{*}P < 0.05$ (unpaired t-test for fluorescent compounds, paired t-test for parent steroids).

test whether diffusion or active transport is responsible for intracellular accumulation we synthesized and imaged the enantiomer of C17-NBD-3α5αA: *ent*-C17-NBD-3α5αA. We compared the enantiomers (0.5 μM) on the same cells using the same protocol for drug application and wash shown in Fig. 6. In all cells imaged, *ent*-C17-NBD-3α5αA showed the same fluorescence profile as C17-NBD-3α5αA, including the unexpected rise in intracellular fluorescence on saline wash (Fig. 8, *A* and *B*). These results suggest that nonspecific diffusion is involved in steroid intracellular accumulation and that selective transport mechanisms are not importantly involved.

In contrast to the cellular accumulation results—but as expected from previous studies of 3α5αP enantioselectivity at GABARs (Covey et al. 2000; Wittmer et al. 1996; Zorumski et al. 1998)—we found in electrophysiology experiments that GABA potentiation by fluorescent enantiomers was highly enantioselective. *Ent*-C17-NBD-3α5αA (0.5 μM) coapplied with GABA exhibited no potentiation (Fig. 8*C*, *black trace*),

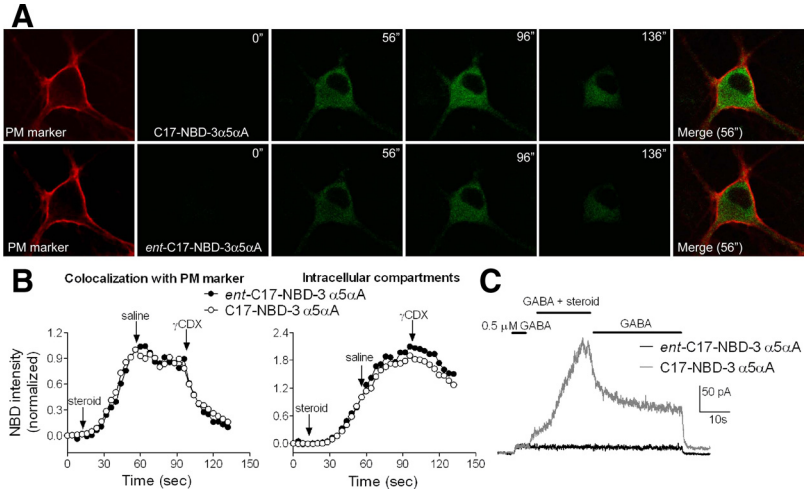

FIG. 8. Comparison of C17-NBD-3α5αA and its enantiomer with respect to cellular accumulation and to GABA response potentiation. *A*: hippocampal neurons were stained with PM marker, and NBD-tagged steroids (0.5 μM) were applied for 40 s. Washes with saline and then with 500 μM γCDX lasted for 40 s (each wash). Images were acquired at 4-s intervals. Similar intracellular accumulation and elimination were observed. Although in this example, *ent*-C17-NBD-3α5αA exhibited somewhat weaker fluorescence than that of its natural counterpart, this was not consistent among all cells; there was no statistical difference in mean fluorescence intensities. Merged images used the NBD-steroid images from the 56″ time point. *B*: fluorescence intensities, normalized to the last point of steroid application, were plotted over time. Traces representative of 6 cells are shown. Start points of drugs application and washes are indicated by arrows. *C*: representative traces (n = 4) showing effects of C17-NBD-3α5αA and its enantiomer (0.5 μM) on GABA (0.5 μM) responses. The enantiomer pair exhibits a strong difference in GABA potentiation.

compared with an equimolar concentration of the natural enantiomer, which robustly potentiated GABA responses (Fig. 8*C*, *gray trace*). The traces in Fig. 8*C* are representative of four cells challenged with both C17-NBD-3α5αA and *ent*-C17-NBD-3α5αA. Together these experiments showed that even if the drug can easily cross the plasma membrane and accumulate indistinguishably from a neuroactive steroid analogue, additional structural features (likely those features involved in binding to a proteinaceous receptor site) are important determinants of GABAR activity.

DISCUSSION

Steroid potency versus affinity

Neurosteroids are of interest partly because of their high potency and strong efficacy in modulating $GABA_AR$ function. However, potency is an empirical concept and may or may not be closely related to site affinity. Our studies show that although potency is high from the perspective of aqueous concentration of steroid analogues, a consequence of a transmembrane domain binding site (Hosie et al. 2006) is that steroid affinity for the GABAR is quite low. If log P of 4 for 3α5αP is taken literally, an aqueous EC_{50} concentration of 100 nM (e.g., as is typical for 3α5αP) corresponds to a membrane concentration potentially as high as 1 mM, likely a closer reflection of the steady-state affinity of the steroid site than potency (aqueous EC_{50}) estimates. If the $GABA_A$ transmembrane domain steroid site had an affinity comparable to that of soluble nuclear steroid receptors (high picomolar to nanomolar k_d), aqueous EC_{50} would be in the femtomolar range. Steroid analogues with otherwise similar binding properties possess different potency and onset/offset kinetics because of differing lipophilicity. This conclusion extends to the two naturally occurring neurosteroids 3α5αP (allopregnanolone) and 3α5αTHDOC.

The major conclusion of the present work outlined here may not be intuitively obvious, but it has profound implications for how a ligand acts at its receptor and how we think about issues of potency and affinity for highly lipophilic agents. Is the fraction of bound receptors at a given aqueous concentration really expected to be different depending on whether the path of steroid is aqueous or membrane delimited and depending on the lipophilicity of ligand? To help conceptualize the issue, we created a simple model of steroid actions. The methods and parameters for the model are given in the Supplemental text and Supplemental Table S1. Figure 9, *A* and *B* shows the response of a receptor to aqueous ligand. The on and off rates of the receptor are set to yield a low-affinity (and low-potency) compound (Fig. 9*B*).

Figure 9, *C* and *D* shows the response of the same receptor when embedded in a compartment (representing the lipid bilayer) into which ligand accumulates over time before binding receptor. The rates of accumulation and departure from the compartment were constrained to yield similar kinetics to those observed for fluorescent steroids. The ratio of the rates was also set to give a departure rate four orders of magnitude slower than the entry rate, yielding a log P value of 4.0, similar to that of 3α5αP. The potency, plotted as a function of aqueous concentration, increased significantly for the membrane-embedded receptor (note the difference scales on the *x*-axis of Fig. 9, *B* and *D*), even though the microscopic affinity rate constants

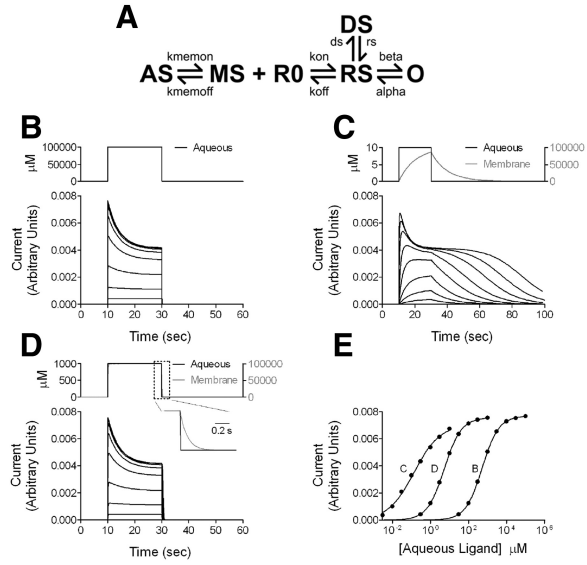

FIG. 9. Simulations of conventional aqueous ligand access vs. membrane access to a receptor. *A*: kinetic scheme for the simulations. See Supplemental text and Supplemental Table S1 for details of the simulation parameters, including rationale and constraints. AS, aqueous steroid ligand; MS, membrane steroid; R0, unbound receptor; RS, ligand bound receptor; O, open channel; DS, a liganded desensitized state. Binding parameters (k_{on}, k_{off}) were set to simulate a low-affinity receptor. Only the open state is conducting. *B*: simulations of a conventional receptor responding to aqueous ligand application. In the context of the scheme shown in *A*, this was implemented by setting $K_{mem\ on}$ and $K_{mem\ off}$ to equal values, more rapid than other rate constants in the scheme. The *bottom* panel shows simulated current responses to a 20-s pulse of aqueous concentrations of applied agonist (concentration range, 30 μM to 100 mM). The *top panel* shows aqueous agonist concentration profile for the largest response. *C*: simulated current responses of a membrane receptor to aqueous application of agonist with a log P of 4 (aqueous concentration range, 0.03–3 μM). Membrane accumulation and departure rates were based on observations from fluorescent steroids; values are given in the Supplemental text. The concentration traces represent aqueous (black) and membrane (gray) concentrations for a 20-s pulse application of 10 μM aqueous ligand, the highest concentration simulated. Note that the asymptotic membrane concentration exceeds the aqueous concentration by 4 orders of magnitude. *D*: the simulation was repeated with membrane departure rate sped 100-fold relative to the simulation in *C* and *D* to simulate a ligand with log P of 2 (aqueous concentration range, 0.3–1,000 μM). Concentration traces again represent the highest concentration simulated (1,000 μM aqueous). The *inset* shows the boxed region and shows the difference between the time courses of aqueous and membrane concentration on aqueous ligand removal. *E*: concentration–response curves for peak responses from the data in *B–D*. The letter associated with each curve represents the relevant panel letter. The solid lines represent fits to the Hill equation. For the data in *B* (receptor for aqueous ligand), the potency (EC_{50}) estimate from the fit was 519.4 μM, with a Hill coefficient of 0.99. For the data in *C* (membrane receptor, ligand log P = 4), the EC_{50} from the fit was 0.14 μM, with a Hill coefficient of 0.64. For the data in *D* (membrane receptor, ligand log P = 2), the fit yielded an EC_{50} of 5.26 μM and a Hill coefficient of 0.97. Note that the dramatic shifts in EC_{50} were effected with no change in ligand binding or dissociation constants, k_{on} and k_{off}.

of the receptor remained the same between the simulation runs. Other features, notably strong dependence of onset and offset times on agonist concentration (cf. Fig. 3*A*), were also quite similar to features of steroid-potentiated responses. To simulate a ligand with lower lipophilicity (e.g., alphadolone), we increased the departure rate constant from the membrane compartment by two orders of magnitude. Rerunning the simulation produced the expected change in potency and offset kinetics (Fig. 9, *E* and *F*). These simulations make it clear that both kinetic and steady-state potency measures are expected to be affected by lipophilicity for a transmembrane receptor.

We cannot completely exclude the possibility that the different structures of the steroids explored also altered the pharmacophore and binding. Indeed, a hydrophobic transmembrane binding site has been proposed to mediate neurosteroid actions (Hosie et al. 2006). However, our analysis of offset kinetics is important to the argument for strong nonspecific lipophilic contributions to steroid potency. Similar to predictions from the simulation (Fig. 9), steroid analogues exhibited graded offset kinetics that varied with lipophilicity. Because offset time of analogue action will also influence the steady-state EC_{50}, analogues with the slowest offset will also yield the lowest EC_{50} values (highest potency). Although slow current offset is typically associated with high receptor affinity (e.g., Lester and Jahr 1992), true affinity differences should not be sensitive to a scavenger of unbound steroid, γCDX. γCDX-dependent speeding of steroid offset kinetics (Fig. 4, *B* and *C*) demonstrates that steroid differences are most strongly governed by nonspecific accumulation differences rather than by affinity differences. Affinity for all the steroid ligands is actually quite weak.

It is also possible that considerations beyond simple log P considerations will affect the nonspecific component of steroid potency. For instance, steroid orientation in the membrane (Makriyannis et al. 2005), membrane lipid composition, intracellular accumulation, and accumulation in surrounding cells including astrocytes may all participate in the nonspecific component, especially in intact brain tissue. From this perspective, it may be surprising that simple log P estimates hold any predictive power.

Observations from fluorescent analogues

Surprisingly, with relatively brief applications (40 s) C17-NBD-3α5αA intracellular fluorescence continued to increase during washout of aqueous analogue. Because the NBD fluorophore is known to be sensitive to the local environment (Kenner and Aboderin 1971; Schneider et al. 1991), we think the most likely explanation for this phenomenon is that during the wash period, C17-NBD-3α5αA slowly redistributes into new intracellular compartments where fluorescence increases. In fact we found that with 2-min (rather than the typical 40-s) application of C17-NBD-3α5αA, fluorescence did not continue to increase (data not shown), suggesting that redistribution equilibrated within this longer exposure time. This redistribution may contribute to the extreme difficulty in washing out the fluorescence and the functional effects of C17-NBD-3α5αA, even with γCDX. Interestingly, the phenomenon appears unique to C17-NBD-3α5αA and its enantiomer. The reason for this peculiar aspect is unclear, but it appears that the 11-ketone group in C17-NBD-alphaxalone allows this steroid to enter into the plasma membrane and transfer to other membrane compartments more rapidly than C17-NBD-3α5αA. In support of this speculation, we observed that cells incubated for 90 min in C17-NBD-3α5αA eventually reached a fluorescence equivalent to that of C17-NBD-alphaxalone (data not shown). The observed fluorescence difference at early time points may suggest that C17-NBD-alphaxalone equilibrates with the same intracellular compartments (resulting in increased fluorescence *during* steroid application) much faster than C17-NBD-3α5αA. Alternatively, because we have not been able to localize steroids to particular intracellular compartments, the two analogues may distribute to different intracellular compartments.

C17-NBD-3α5αA failed to show an immediate decrease in fluorescence in perimembrane regions of the cell with wash, despite the fact that GABA potentiation showed an immediate decrease on wash. This suggests that imaging failed to resolve fluorescence in the plasma membrane compartment most directly associated with GABAR modulation. This could be partly because intracellular C17-NBD-3α5αA fluorescence, which continued to increase on wash, was sufficiently bright and resistant to wash that it contaminated our perimembrane measurements, despite our use of confocal planes. This explanation seems likely because C17-NBD-alphaxalone, which did not exhibit the anomalous increase in intracellular fluorescence on wash, exhibited an immediate wash-induced decrease in perimembrane fluorescence that better matched the electrophysiology results.

The similarity in fluorescence behavior of the enantiomer of C17-NBD-3α5αA and its natural counterpart suggests two important conclusions. First, the rapid intracellular accumulation of steroid analogues does not appear to depend on enantiospecific interaction of the steroids with plasma membrane transporters, enzymes, or other proteins. Enantioselectivity is predicted in the case of a proteinaceous binding site because proteins are composed entirely of amino acids in the L-configuration. Instead, the rapid accumulation appears to depend simply on physicochemical properties, which are identical between enantiomer pairs. The rapid accumulation presumably depends on contiguous lipophilic passages between the plasma membrane and intracellular compartments (Voeltz et al. 2002), since we would not expect the steroid to "prefer" to traverse the aqueous cytoplasm to access the cell interior. Second, the identical behavior of the enantiomer with regard to cellular accumulation contrasts markedly with the lack of functional effects on the GABAR. This result demonstrates that in addition to nonspecific membrane interaction, an enantioselective binding site is also involved. Therefore we are not arguing for the old idea that anesthetic action is dictated by membrane fluidity or other affected membrane properties. Our argument is more nuanced. Certainly lipophilicity does not completely explain neurosteroid potency and enantioselective protein–ligand interactions, albeit of low affinity, are also essential. It was also recently shown that 5α-reduced steroids behave differently in membranes than 5β-reduced steroids (Alakoskela et al. 2007), despite identical predicted log P values (and similar reported potencies). Therefore it is also possible that interactions between steroids and the plasma membrane beyond those predicted by simple lipophilicity could be important in the access of steroids to their site(s).

Our results suggest that intracellular steroid pools can affect the longevity of GABA response potentiation. After rapid removal of perireceptor steroid, highly lipophilic steroids such as C17-NBD-3α5αA and 3α5αP slowly redistribute from intracellular compartments to generate a rebound potentiation. Therefore the prolonged offset kinetics of lipophilic steroids likely arises partly from steroid redistribution.

Our experiments (Figs. 2 and 3) also reveal a difference in steroid potency between oocytes and hippocampal neurons. Although several factors might contribute to this difference (different subunit combinations, modulating proteins, second-messenger effects, membrane composition, or intracellular

accumulation), we have previously found that potency of 3α5αP at the α1β2γ2L subunit combination in HEK cells (Li et al. 2007) is more similar to that in neurons than to α1β2γ2L receptors in oocytes. This makes it unlikely that subunit combination explains the difference in potency. It is tempting to speculate that membrane composition differences and resulting differences in steroid solubility could participate.

One important implication of our results is that two natural steroids 3α5αP and 3α5αTHDOC differ in kinetics and these effects correlated with significantly different log P values. Neurosteroids are thought to be synthesized by principal cells of the nervous system (Agis-Balboa et al. 2006) and studies examining steroid localization with an antibody against 5α-reduced steroids suggest strong intracellular and cytoplasmic accumulation in these cells akin to the distribution of the tagged steroids observed here (Saalmann et al. 2007). Thus neurosteroids are well positioned to modulate local activity of principal neurons and factors that regulate intracellular and membrane accumulation may be critical for understanding these actions. Our results predict that 3α5αP might likely serve a predominantly autocrine function, by virtue of being "trapped" in membrane compartments of the cell in which it is synthesized. 3α5αTHDOC may be more likely to traverse aqueous media to have paracrine effects on surrounding cells. Furthermore, we would expect the effects of 3α5αP to have a longer half-life of action because of its stronger lipophilicity.

Neurosteroids regulate the actions of the most widespread inhibitory neurotransmitter in the nervous system—GABA. Our work highlights that nonspecific features of steroid structure such as lipophilicity and intracellular accumulation/distribution help dictate the degree of positive modulation observed, the lifetime of action, and possibly the spatial extent of steroid action at GABARs. Considering these nonspecific characteristics of modulator action will improve drug design, pharmaceutical formulation, and dosage considerations in both research and therapy contexts.

ACKNOWLEDGMENTS

We thank lab members for support and discussion and Dr. Dave Reichert for help with statistics.

GRANTS

This work was supported by National Institutes of Health Grants GM-47969 to D. F. Covey and C. F. Zorumski and NS-54174 to S. Mennerick.

REFERENCES

Adam JM, Bennett DJ, Bom A, Clark JK, Feilden H, Hutchinson EJ, Palin R, Prosser A, Rees DC, Rosair GM, Stevenson D, Tarver GJ, Zhang MQ. Cyclodextrin-derived host molecules as reversal agents for the neuromuscular blocker rocuronium bromide: synthesis and structure–activity relationships. *J Med Chem* 45: 1806–1816, 2002.

Agis-Balboa RC, Pinna G, Zhubi A, Maloku E, Veldic M, Costa E, Guidotti A. Characterization of brain neurons that express enzymes mediating neurosteroid biosynthesis. *Proc Natl Acad Sci USA* 103: 14602–14607, 2006.

Akk G, Covey DF, Evers AS, Steinbach JH, Zorumski CF, Mennerick S. Mechanisms of neurosteroid interactions with $GABA_A$ receptors. *Pharmacol Ther* 116: 35–57, 2007.

Akk G, Shu HJ, Wang C, Steinbach JH, Zorumski CF, Covey DF, Mennerick S. Neurosteroid access to the $GABA_A$ receptor. *J Neurosci* 25: 11605–11613, 2005.

Alakoskela JM, Covey DF, Kinnunen PK. Lack of enantiomeric specificity in the effects of anesthetic steroids on lipid bilayers. *Biochim Biophys Acta* 1768: 131–145, 2007.

Belelli D, Herd MB, Mitchell EA, Peden DR, Vardy AW, Gentet L, Lambert JJ. Neuroactive steroids and inhibitory neurotransmission: mechanisms of action and physiological relevance. *Neuroscience* 138: 821–829, 2006.

Colquhoun D, Large WA, Rang HP. An analysis of the action of a false transmitter at the neuromuscular junction. *J Physiol* 266: 361–395, 1977.

Covey DF, Nathan D, Kalkbrenner M, Nilsson KR, Hu Y, Zorumski CF, Evers AS. Enantioselectivity of pregnanolone-induced γ-aminobutyric $acid_A$ receptor modulation and anesthesia. *J Pharmacol Exp Ther* 293: 1009–1016, 2000.

de Boer HD, van Egmond J, van de Pol F, Bom A, Booij LH. Reversal of profound rocuronium neuromuscular blockade by sugammadex in anesthetized rhesus monkeys. *Anesthesiology* 104: 718–723, 2006.

Gasior M, Carter RB, Witkin JM. Neuroactive steroids: potential therapeutic use in neurological and psychiatric disorders. *Trends Pharmacol Sci* 20: 107–112, 1999.

Gutfreund H. *Kinetics for the Life Sciences: Receptors, Transmitters, and Catalysts.* Cambridge, UK: Cambridge Univ. Press, 1995, p. 346.

Hosie AM, Clarke L, da Silva H, Smart TG. Conserved site for neurosteroid modulation of $GABA_A$ receptors. *Neuropharmacology* 56: 149–154, 2009.

Hosie AM, Wilkins ME, da Silva HMA, Smart TG. Endogenous neurosteroids regulate $GABA_A$ receptors via two discrete transmembrane sites. *Nature* 444: 486–489, 2006.

Jones MV, Sahara Y, Dzubay JA, Westbrook GL. Defining affinity with the $GABA_A$ receptor. *J Neurosci* 18: 8590–8604, 1998.

Kenner RA, Aboderin AA. A new fluorescent probe for protein and nucleoprotein conformation. Binding of 7-(*p*-methoxybenzylamino)-4-nitrobenzoxadiazole to bovine trypsinogen and bacterial ribosomes. *Biochemistry* 10: 4433–4440, 1971.

Lester RA, Jahr CE. NMDA channel behavior depends on agonist affinity. *J Neurosci* 12: 635–643, 1992.

Li P, Shu HJ, Wang C, Mennerick S, Zorumski CF, Covey DF, Steinbach JH, Akk G. Neurosteroid migration to intracellular compartments reduces steroid concentration in the membrane and diminishes $GABA_A$ receptor potentiation. *J Physiol* 584: 789–800, 2007.

Makriyannis A, Tian X, Guo J. How lipophilic cannabinergic ligands reach their receptor sites. *Prostag Other Lipid Mediat* 77: 210–218, 2005.

Mennerick S, He Y, Jiang X, Manion B, Wang M, Shute AA, Benz A, Evers AS, Covey DF, Zorumski C. Selective antagonism of 5a-reduced neurosteroid potentiation of $GABA_A$ receptors. *Mol Pharmacol* 65: 1191–1197, 2004.

Nadeson R, Goodchild CS. Antinociceptive properties of neurosteroids. III: Experiments with alphadolone given intravenously, intraperitoneally, and intragastrically. *Br J Anaesth* 86: 704–708, 2001.

Pytel M, Mercik K, Mozrzymas JW. Interaction between cyclodextrin and neuronal membrane results in modulation of $GABA_A$ receptor conformational transitions. *Br J Pharmacol* 148: 413–422, 2006.

Saalmann YB, Kirkcaldie MT, Waldron S, Calford MB. Cellular distribution of the $GABA_A$ receptor-modulating 3alpha-hydroxy, 5alpha-reduced pregnane steroids in the adult rat brain. *J Neuroendocrinol* 19: 272–284, 2007.

Schneider S, Schramm U, Schreyer A, Buscher HP, Gerok W, Kurz G. Fluorescent derivatives of bile salts. I. Synthesis and properties of NBD-amino derivatives of bile salts. *J Lipid Res* 32: 1755–1767, 1991.

Shu HJ, Eisenman LN, Jinadasa D, Covey DF, Zorumski CF, Mennerick S. Slow actions of neuroactive steroids at $GABA_A$ receptors. *J Neurosci* 24: 6667–6675, 2004.

Shu HJ, Zeng CM, Wang C, Covey DF, Zorumski CF, Mennerick S. Cyclodextrins sequester neuroactive steroids and differentiate mechanisms that rate limit steroid actions. *Br J Pharmacol* 150: 164–175, 2007.

Voeltz GK, Rolls MM, Rapoport TA. Structural organization of the endoplasmic reticulum. *EMBO Rep* 3: 944–950, 2002.

Westover EJ, Covey DF. The enantiomer of cholesterol. *J Membr Biol* 202: 61–72, 2004.

Wittmer LL, Hu Y, Kalkbrenner M, Evers AS, Zorumski CF, Covey DF. Enantioselectivity of steroid-induced γ-aminobutyric $acid_A$ receptor modulation and anesthesia. *Mol Pharmacol* 50: 1581–1586, 1996.

Zorumski CF, Mennerick S, Isenberg KE, Covey DF. Potential clinical uses of neuroactive steroids. *Curr Opin Investig Drugs* 1: 360–369, 2000.

Zorumski CF, Mennerick SJ, Covey DF. Enantioselective modulation of GABAergic synaptic transmission by steroids and benz[e]indenes in hippocampal microcultures. *Synapse* 29: 162–171, 1998.